Original Paper

Cells Tissues Organs

Cells Tissues Organs 2002;171:99–116

Received: February 26, 2001
Accepted after revision: October 10, 2001

The PICM-19 Cell Line as an in vitro Model of Liver Bile Ductules: Effects of cAMP Inducers, Biopeptides and pH

Neil C. Talbot Thomas J. Caperna Kevin D. Wells

US Department of Agriculture, Agricultural Research Service, Beltsville, Md., USA

Key Words
Bile duct · Liver · Stem cells · Cell culture · Pig

Abstract
The PICM-19 fetal liver cell line was isolated from the primary culture and spontaneous differentiation of pig epiblast cells, i.e. embryonic stem cells. PICM-19 cells were induced to differentiate into mostly ductular formations by culturing at pH 7.6–7.8. The ductules were functionally assayed by treatment with cAMP inducing agents and bioactive peptides reported to influence the secretory activity of liver bile ductules. The secretory response of the cells was assessed by qualitative or quantitative measurement of the cross-sectional area of the ductal lumens and the appearance of biliary canaliculi in between PICM-19 cells that had formed monolayers instead of ducts. Forskolin (10 μ*M*) and 8-bromoadenosine 3′:5′-cyclic monophosphate (bcAMP; 2 m*M*) stimulated fluid transport and expansion of ductal structures in 15–20 min and stimulated the appearance and expansion of biliary canaliculi in 30–60 min. Cholera toxin (50 ng/ml) stimulates fluid transport in both ductules and canaliculi in 1–2 h, while 8-bromoguanosine 3′:5′-cyclic monophosphate (bcGMP; 2 m*M*) stimulated only biliary canaliculi in 2 h. Glucagon (1.4 n*M*) produced a similar response in 5–10 min in ductal structures only, but the response was transitory and was almost completely reversed within 30 min. Secretin (100 p*M*) and vasoactive intestinal peptide (75 p*M*) produced a sustained response with maximal ductal lumen expansion occurring in 5–10 min and neither had an immediate effect on canaliculi. Somatostatin (0.5 μ*M*) and gastrin (1 μ*M*) caused marked reduction or disappearance of ductal lumens in 30–60 min, but was ineffective in reversing secretin (100 n*M*)-induced

Abbreviations used in this paper

bcAMP	8-bromoadenosine 3′:5′-cyclic monophosphate
bcGMP	8-bromoguanosine 3′:5′-cyclic monophosphate
BME	β-mercaptoethanol
BSA	bovine serum albumin
CCK-8	cholecystokinin
dbcAMP	N^6,2′-O-dibutyryladenosine 3′:5′-cyclic monophosphate
dbcGMP	N^2,2′-O-dibutyrylguanosine 3′:5′-cyclic monophosphate
DMEM	Dulbecco's modified Eagle's medium
FBS	fetal bovine serum
GGT	γ-glutamyl transpeptidase
PBS	Dulbecco's phosphate-buffered saline
RBC	red blood cell
STO	SIM mouse, thioguanine- and ouabain-resistant
TEM	transmission electron microscopy
VIP	vasoactive intestinal peptide
199	Medium 199

KARGER

Fax + 41 61 306 12 34
E-Mail karger@karger.ch
www.karger.com

1422–6405/02/1713–0099$18.50/0

Accessible online at:
www.karger.com/journals/cto

Neil C. Talbot
USDA, ARS, ANRI, GEML
Bldg. 200, Rm. 13, BARC-East
Beltsville, MD 20705 (USA)
Tel. +1 301 504 8216, Fax +1 301 504 8414, E-Mail Ntalbot@anri.barc.usda.gov

duct distension. Application of the adrenergic agonists, epinephrine, isoproterenol, and phenylephrine (100 μ*M*), resulted in the complete shrinkage of ductal lumens in 20–30 min. A shift to pH 7.0–7.2 resulted in almost complete reduction of ductal lumens, while a shift to pH 7.8–8.0 resulted in expansion, although not full expansion, of the ductal lumens. PICM-19 bile duct cultures were positive for cytokeratin-7, aquaporin-1 and aquaporin-9 by Western blot analysis. The amounts of these proteins increased in the cultures as differentiation proceeded over time. Transmission electron microscopy revealed that the ductal structures were usually sandwiched between SIM mouse, thioguanine- and ouabain-resistant (STO) feeder cells that had produced a collagen matrix. Also, the ductular PICM-19 cells possessed cilia, probably occurring as a single cilium in each cell, that projected into the lumens of the ducts. The results indicated that the in vitro-produced ductal structures of the PICM-19 cell line are a functional model for biliary epithelium.

Introduction

The in vitro culture of the totipotent embryonic stem cells of the preimplantation pig blastocyst, the epiblast cells, resulted in the isolation of a specific differentiated cell type that either formed monolayers of cuboidal cells with distinct round nuclei or multicellular cord-like structures composed of columnar-like epithelium [Talbot et al., 1993, 1994a, b]. One of these cultures, designated PICM-19, was established as a cell line. That is, the cells can be cloned without loss of character and division potential. The PICM-19 cultures were found to have both inducible P-450 activity, a marker of hepatocytes, and high γ-glutamyl transpeptidase (GGT) activity, a marker of bile duct epithelium [Talbot et al., 1996]. They also expressed α-fetoprotein along with albumin and other liver-specific proteins [Talbot et al., 1996]. Besides these markers, the SIM mouse, thioguanine- and ouabain-resistant (STO) co-culture of numerous tissues of fetal and adult pigs (e.g., testis, kidney, pancreas, lung, brain, intestine, mammary gland, muscle, skin and blood) have not yielded cells that are similar in appearance or behavior to the PICM-19 cells. In contrast, the culture of fetal pig liver tissue [Talbot et al., 1994b] and adult pig liver tissue [Talbot et al., 1998] resulted in cell cultures that closely resembled the PICM-19 cells morphologically and biochemically. Thus, the PICM-19 cells appear to be bipotent liver stem cells with the ability to differentiate into monolayers of hepatocytes or multicellular ductal structures resembling bile duct epithelium.

As will be demonstrated here, the PICM-19 cells can be induced towards one differentiated phenotype or the other by the pH at which the cells are maintained during static culture, i.e. refeeding of the cells over 3–4 weeks of culture without further dissociation. Approximately 75% of the cells in the culture will differentiate into multicellular ductal structures under static culture conditions of pH 7.6–7.8. The present investigation was also undertaken to provide further structural and functional evidence of the bile duct character of the in vitro-produced PICM-19 ductal structures, since their derivation from embryonic stem cells carries a higher burden of proof. The significance of the PICM-19 cell line as an in vitro model of bile duct epithelium is discussed.

Materials and Methods

Cell Culture and Reagents

All cells were grown on 25-cm^2 tissue culture flasks (Greiner, Frickenhausen, Germany). Fetal bovine serum (FBS) was purchased from Hyclone (Logan, Utah). Cell culture reagents including Dulbecco's phosphate-buffered saline (PBS) without Ca^{2+} and Mg^{2+}, media, trypsin-EDTA (0.025% trypsin, 0.43 m*M* EDTA), antibiotics, nonessential amino acids, and *L*-glutamine were purchased from Gibco (Gaithersburg, Md.).

The derivation and continuous culture of the PICM-19 cell line were previously described [Talbot et al., 1993, 1994a]. PICM-19 cells were grown on irradiated (8 kRad) STO mouse fibroblast (CRL 1503, American Type Culture Collection, Rockville, Md.) feeder cell layers, or, when indicated, mitomycin C-treated STO feeder cells [Talbot and Paape, 1996]. The growth and differentiation medium [50:50 ratio of Dulbecco's modified Eagle's medium-Medium 199 (DMEM-199) with 10% FBS supplementation; Talbot and Paape, 1996] was modified to equilibrate at pH 7.6–7.8 in 5% CO_2 by the addition of extra sodium bicarbonate (3.7 g/l final concentration) to induce multicellular ductal differentiation in the majority of the PICM-19 cells over 3–4 weeks of static culture, i.e. without passage of the cells and with refeeding every 3–4 days. Cultures of nearly pure pig bile duct epithelium derived from adult pig liver tissue were used for comparative purposes in some assays, and they were grown and maintained on STO feeder cells as previously described [Talbot and Caperna, 1998].

Endothelin-1 was purchased from Calbiochem (San Diego, Calif.). Bioactive peptides, forskolin and cholera toxin were purchased from Sigma Chemical Co. (St. Louis, Mo.), and were dissolved in TL-HEPES solution (BioWhittaker, Walkersville, Md.) or PBS for making concentrated stock solutions. N^6,2′-O-dibutyryladenosine 3′:5′-cyclic monophosphate (dbcAMP), N^2,2′-O-dibutyrylguanosine 3′:5′-cyclic monophosphate (dbcGMP), and the phosphodiesterase-resistant analogues, 8-bromoadenosine 3′:5′-cyclic monophosphate (bcAMP) and 8-bromoguanosine 3′:5′-cyclic monophosphate (bcGMP), were also obtained from Sigma and were prepared at

2 m*M* in 10% DMEM-199 medium. Biochemicals for Western blotting were obtained from Sigma or from BioRad (Hercules, Calif.). Colcemid was purchased from Gibco.

Assay of GGT Activity and P-450 Levels

T25 cultures of PICM-19 cells were grown under either high (7.8–8.0) or low (6.9–7.1) pH static culture conditions for 4 weeks (achieved by adjusting the CO_2 levels in separate incubators). STO feeder cells were prepared by mitomycin C (Sigma) inactivation as previously described [Talbot and Paape, 1996]. PICM-19 cocultures were harvested at several time points postpassage for whole-cell homogenates and microsomes. Two days prior to harvest the cultures were exposed to metyrapone to stimulate P-450 expression. P-450 levels and GGT activity were determined as previously described [Talbot et al., 1996] from a pool of three flasks for each time point assayed.

Phase-Contrast Microscopic Evaluation of Ductular Fluid Transport

For assessing the effects of culture conditions, chemical reagents, and bioactive peptides on the fluid transport by PICM-19 ductal structures, five areas approximately 1 mm × 1 mm in size were delineated by marking the bottom of the flask with an ultrafine tipped Sharpie marking pen. The ductules in these five areas were observed and an approximation made of their maximal positive or negative response, – = no response to ++++ = maximum response, in respect to the cross-sectional area of their lumens. The appearance or disappearance of canaliculi between hepatocyte-like monolayer formations of PICM-19 cells was also assessed if they were present in the delineated area. The number of observations made in the five areas over time depended on the speed of the response. For example, for 10 n*M* secretin the five areas were visually assessed every 1–2 min, for 500 n*M* somatostatin the five areas were assessed every 5 min, and for acidic pH shifts the five areas were assessed every 10–15 min. The duration of responses, when noted, was ascertained by washing the cultures 3 times with medium after a maximal response had been achieved.

Microscope Image Analysis

PICM-19 ductule lumen diameters were measured from calibrated images collected at 20-second intervals using MetaMorph Imaging System version 3.6 (West Chester, Pa.).

Transmission Electron Microscopy

Transmission electron microscopy (TEM) sample preparation and photomicroscopy were done with the assistance of JFE Enterprises (Brookeville, Md.) as previously described [Talbot et al., 1998, 2000]. Ultrastructural analysis was performed on samples processed from two T-25 flask cultures that were 6 weeks postpassage. One flask was treated with 100 n*M* secretin for 10 min prior to fixation to stimulate fluid transport and ductular expansion. The other flask was not stimulated and most ductules were in a fully collapsed state. An area that was observed to be fully collapsed prior to fixation was specifically delineated for sectioning.

Western and Immunoblotting Analysis of PICM-19 Protein Expression

PICM-19 cells were seeded into T-25 flasks and cultured as described above. At various times postpassage, medium was removed and flasks were washed 3 times with PBS at 4°C. Cells from duplicate flasks were scraped in buffer, containing 20 m*M* Tris, 1 m*M* β-mercaptoethanol (BME), 0.005% aprotinin, and 10% glycerol, pH 7.5 (TBAG) and frozen at –30°C. For comparative purposes, STO feeder cells alone, cystic duct and interlobule bile duct tissue, whole liver tissue, and red blood cells (RBC) were collected from a normal pig. Tissues were minced in 20 m*M* Tris buffer containing 1% KCl, 0.005% aprotinin and 1 m*M* BME, pH 7.5 (TBAK), homogenized mechanically (Omni 2000, Omni, Waterbury, Conn.), briefly sonicated with a microprobe (Model XL, Misonix, Farmingdale, N.Y.) and centrifuged at 105,000 *g* for 30 min at 4°C. Supernatants were aspirated and membranes were resuspended in TBAG buffer by sonication. Red cell membranes were obtained by repeatedly washing whole blood cells (collected in the presence of EDTA) in normal saline to remove plasma and leukocytes and by final sonication in TBAK buffer. Sonicated material was centrifuged at 105,000 *g* and the pellet was resuspended in the TBAK. Membranes were centrifuged and washed 2 additional times prior to resuspension in TBAG buffer. Cell lysates and membrane material were sonicated prior to analysis of protein concentration by a modified Lowry procedure [Nerurkar et al., 1981], using bovine albumin as standard.

Cell lysates and membrane fractions were separated by SDS-PAGE (Mini Protean-3, BioRad, Hercules, Calif.) and were blotted onto 0.2-μm pore nitrocellulose using a semidry blotting system (BioRad). All samples were boiled (5 min) in gel loading buffer containing 62.5 m*M* Tris, 1 m*M* EDTA, 5% BME, 6% glycerol and 1.5% SDS, pH 7.0. Eighteen micrograms of protein in 40 μl were loaded in each lane of 1.5-mm-thick, 12% acrylamide gels. Following electrophoresis and electrotransfer onto nitrocellulose, blots were stained with fast green to visualize total proteins. Blots were blocked for nonspecific reactions by overnight incubation in Tris-saline containing 3% bovine serum albumin (BSA; Sigma, A7888) and 3% nonfat dry milk (Carnation, Nestlé Food, Glendale, Calif.). After washing, blots were incubated with mouse anti-cytokeratin-7 (1/750, clone OVTL 12–30 CAPPEL Research Products, Durham, N.C.) and affinity-purified rabbit anti-aquaporin-1 or anti-aquaporin-9 (1/1222, Alpha Diagnostics, San Antonio, Tex.) for 3 h in Tris saline containing 0.5% BSA, 0.5% gelatin and 0.05% Tween 20. Alkaline phosphatase-conjugated secondary antispecies antibodies (Sigma; A2256 and A2179) were applied in the same buffer for 1.5 h. The presence of specific proteins was evaluated by a colorimetric alkaline phosphatase detection system (BCIP/NBT, Sigma, St. Louis, Mo.). Stained nitrocellulose blots were scanned with a digital imaging system (Chemimager 4000, Alpha Innotech Corp., San Leandro, Calif.).

Results

Growth and Differentiation of PICM-19 Cells at pH 7.6–7.8

Static culture, i.e. refeeding every 3–4 days for a period of 1–2 months, of PICM-19 cells at pH 7.6–7.8, resulted in the preferential differentiation of the cells so that the majority of the cells participated in the formation of multicellular ductal structures. Assay of total P-450 levels and GGT activity in PICM-19 cells cultured under differential pH conditions showed that PICM-19 cultured in high pH conditions had relatively elevated GGT and low-

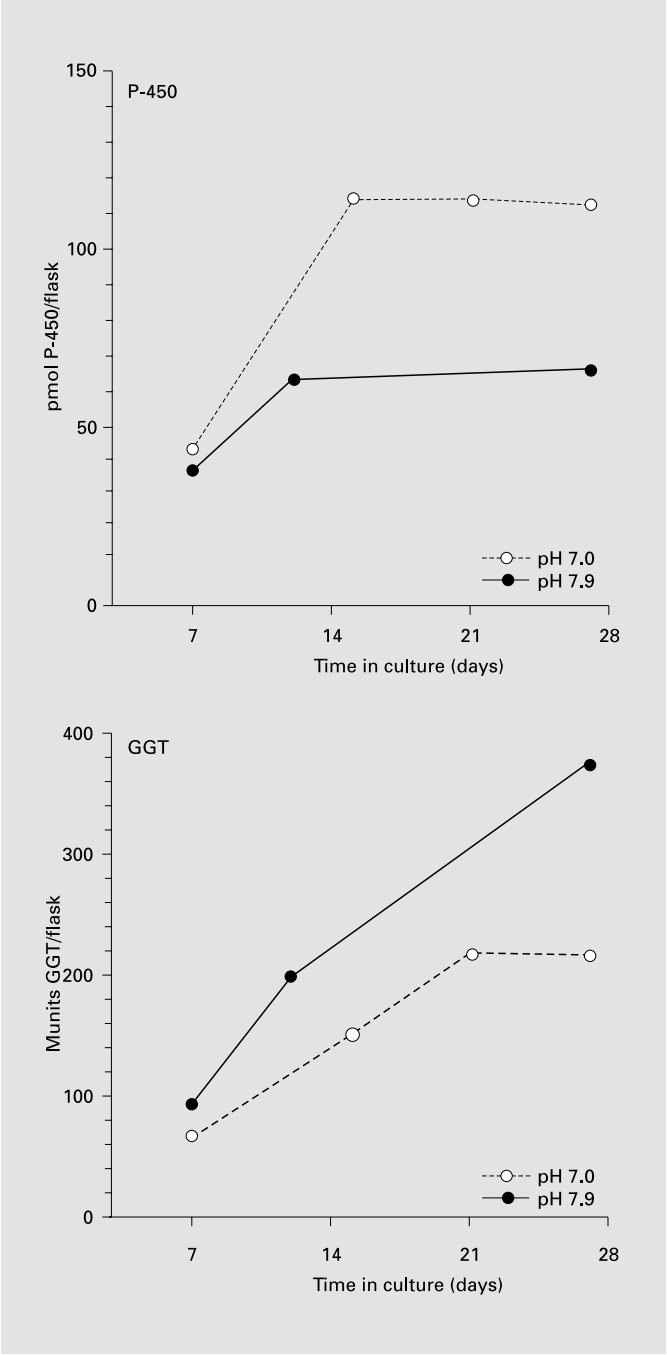

Fig. 1. PICM-19 cells cultured under different pH conditions: influence on P-450 levels and GGT activity. PICM-19 cells were grown in standard culture medium (see Materials and Methods) and the pH of the culture conditions was adjusted by altering the CO_2 level in two incubators. Two days prior to harvest, metyrapone (0.5 m*M*) was added to each culture flask (each point represents a pool of three T-25 flasks). At the indicated times microsomes were prepared from the cells and P-450 content was determined spectrophotometrically. GGT activity was determined from whole cell homogenates. GGT and P-450 were undetectable in STO cells [not shown; Talbot et al., 1996].

ered P-450 by 3–4 weeks postpassage compared to those maintained at lower pH (fig. 1). It was estimated by microscopic observation that 70–90% of the cells were found in ductal structures by the 6th week of static culture (fig. 2). The remaining PICM-19 cells formed small monolayer patches of hepatocyte-like cells, i.e. larger cuboidal cells with distinct large nuclei and canaliculi occurring here and there between the cells. Also, some of these hepatocyte-like cells had large lipid droplets associated with them (fig. 2) [Talbot et al., 1994a]. After 4–6 weeks at high pH, the PICM-19 cultures could be refed with 10% DMEM/199 containing the standard amount of bicarbonate (Gibco) so that the pH was about 7.4 thereafter. This improved the long-term maintenance of the cells, and they retained form and function out to 3 months of culture. By this method numerous mass cultures of multicellular ductal structures could be routinely produced for subsequent experimentation.

Induction of Lumen Fluid Transport by cAMP Inducers, Bioactive Peptides and pH

The PICM-19 multicellular ductal structures were observed to be dynamic. That is, their lumens were observed to swell or deflate (to the point of disappearing) over time in culture. It was observed that the external pH, i.e. the pH of the medium, had a marked influence on PICM-19 ductular fluid transport. If the pH of the medium was raised (by the addition of ambient air to the flask) to approximately pH 7.6–8.0, positive fluid transport occurred, i.e. transport of fluid into the ducts occurred and their lumens increased in cross-sectional area over 15–30 min (fig. 3). Conversely, if the pH of the medium was lowered (by the addition of CO_2 to the flask) to approximately 6.9–7.1, negative fluid transport, i.e. transport out of the ductule, occurred in 60–90 min (fig. 3). The lumen of the ductal structure would disappear completely, and the cells became more rounded and less organized in their orientation to each other in this instance.

The influence of various agents known to increase cAMP within cells was tested at a constant and approximate pH of 7.3–7.4. If the pH was not maintained at these physiological levels, the effective dose response and time of the response were negatively or positively affected in accordance with the pH effects described above. Refeeding the cultures with fresh medium had no apparent effect, immediately or within several hours, on fluid transport into or out of the ductules. Also, adding carrier buffer (TL-HEPES) alone had no effect on the fluid transport response of the ductal structures over several hours.

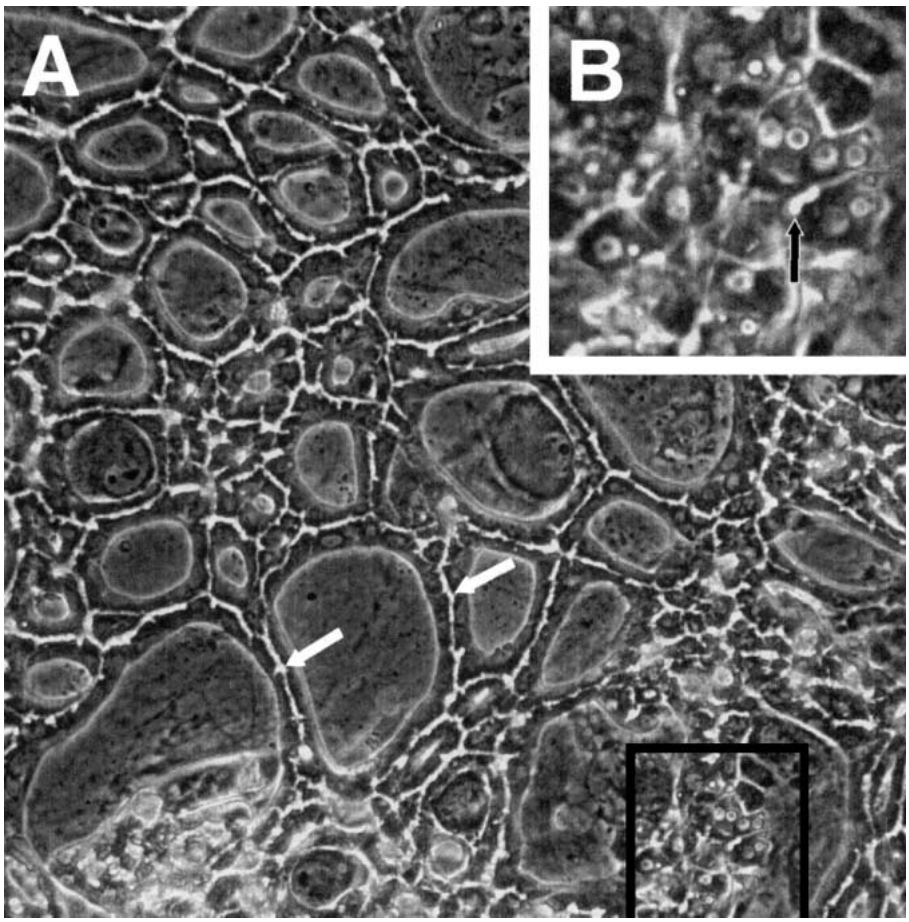

Fig. 2. Phase-contrast micrograph of PICM-19 cells after 4 weeks of pH 7.6–7.8 culture and an additional 7 weeks in culture at pH 7.4. Note that most of the PICM-19 cells (A) have differentiated into ductal structures (arrows indicate the lumens of the ducts). A few 'hepatocyte-like' PICM-19 cells can be seen (delineated by the black box) and enlarged in the inset (B). Note the canaliculi (arrow) connecting the cells and the large lipid droplets within them. × 30.

PICM-19 cultures that had undergone static culture to induce differentiation into multicellular ductal structures were assayed for their responsiveness to cAMP-inducing agents reported to affect bile secretion or fluid transport in bile duct epithelium. The secretory response of the cells was assessed by the appearance of and cross-sectional measurement of the lumen in ductal structures. Also, their effect on the canaliculi occurring in monolayers of hepatocyte-like PICM-19 cells was noted. Forskolin (10 μ*M*) and bcAMP (2 m*M*) stimulated fluid transport and expansion of ductal structures in 15–20 min and stimulated the appearance and expansion of biliary canaliculi in 30–60 min (table 1, fig. 4). Cholera toxin (50 ng/ml) stimulated fluid transport in both ductules and canaliculi in 1–2 h and gave a particularly sustained response, while bcGMP (2 m*M*) stimulated only biliary canaliculi in 2 h (table 1). The cyclic nucleotide analogs, dbcAMP (1 or 2 m*M*) and dbcGMP (2 m*M*), produced relatively weak or no responses, respectively, after 2–3 h (table 1). A similar response to forskolin was found in pig liver-derived bile duct tissue cultures [Talbot and Caperna, 1998] which were tested as a comparative control (table 4).

The in vitro-produced ductal structures were exposed to bioactive peptides reported to influence the secretory activity of liver bile ductules (tables 1, 2, fig. 5–7). Porcine secretin (≥100 p*M*) and vasoactive intestinal peptide (≥75 p*M*) produced a sustained response with maximal lumen expansion occurring in 5–10 min in ductal structures, and canaliculi between hepatocyte-like cells were either not effected or expanded much later over a 30- to 60-min period. Secretin at 1 p*M* produced a 50% response (in all five independent areas inspected) over a 20- to 30-min period. The secretin response was not inhibited by a prior 1-hour exposure of the cells to colcemid indicating that microtubule trafficking was not essential. Glucagon (1.4 n*M*) produced a similar response (in ~ 5 min) in ductal structures only, but the response was transitory, being almost completely reversed within 30 min. Bombesin (1 μ*M*), neuropeptide Y (0.1 μ*M*), cholecystokinin (CCK-8; 1–10 μ*M*), vasopressin (1 IU) and endothelin-1

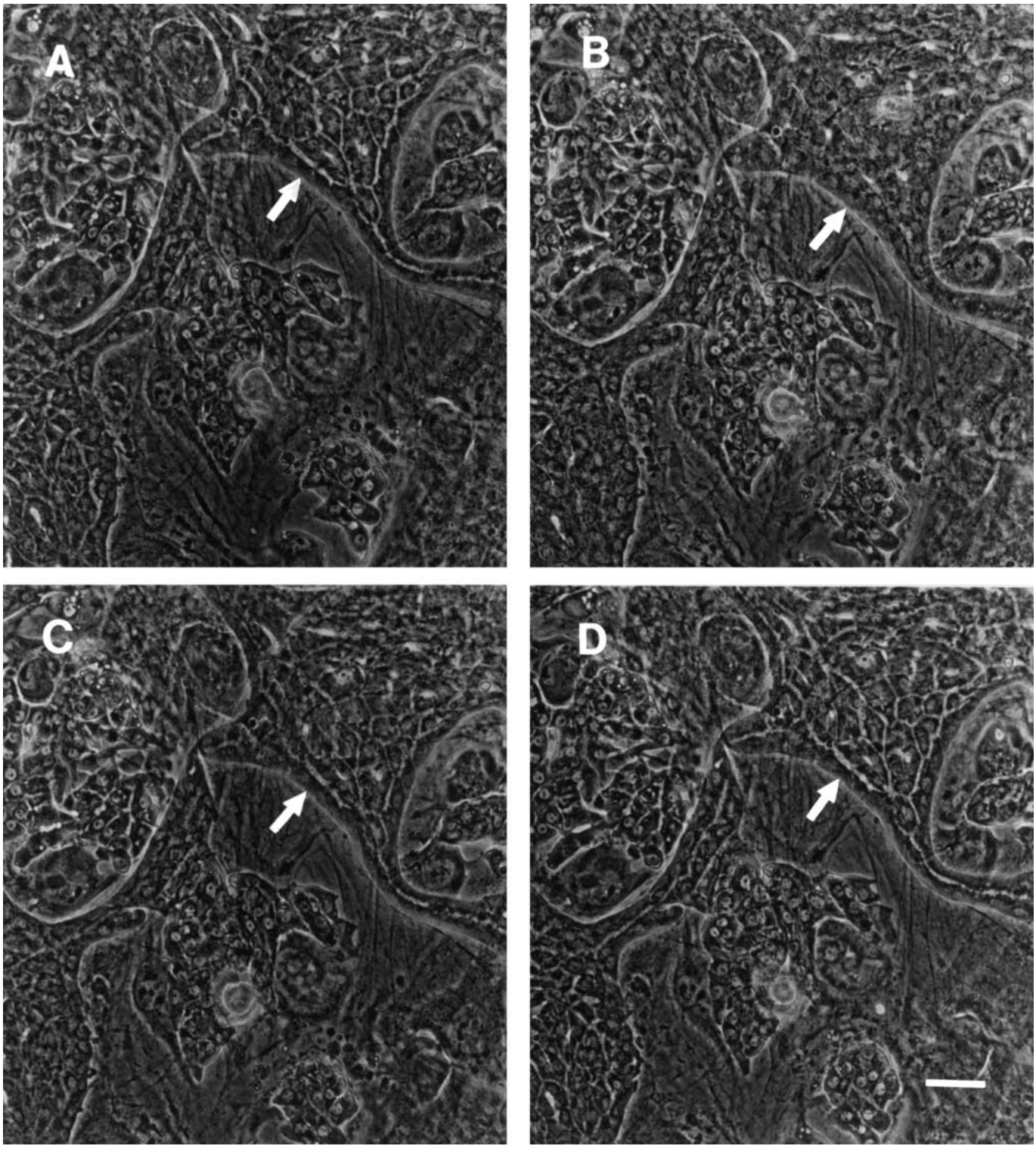

Fig. 3. Phase-contrast micrographs of the response of PICM-19 hepatocyte-like cell monolayers and ductal structures to changes in culture medium pH. A Starting configuration of the cells at ~pH 7.4. B Same area after shifting medium to ~ pH 7.1 for 30 min. C Same area after shifting from ~ pH 7.1 to ~pH 7.8 for 20 min. D Same area after 60 min at ~pH 7.8. Note that the ductal structure lumens (arrows) collapsed as the external pH was made relatively acidic (B) and then reexpanded when the external pH was made relatively basic (C, D). Bar ≈40 μm.

Table 1. Positive fluid transport response of PICM-19 biliary canaliculi and ductules to cAMP inducers, bioactive peptides and elevated pH

Peptides/ cAMP inducers	Biliary canaliculi	Biliary ductules	Dosage tested	Response time	Duration of response
Cholera toxin	++++	++++	50 ng/ml	60–90 min	12–24 h
Forskolin	++++	++++	10 μ*M*	10–20 min	1–2 h
dbcAMP	++	++	1–2 m*M*	2–4 h	ND
bcAMP	+++	++++	2 m*M*	10–20 min	3–4 h
dbcGMP	–	–	2 m*M*	N/A	N/A
bcGMP	++++	–	2 m*M*	90–120 min	5–6 h
Glucagon[a]	+/–	+++	1.4–143 n*M*	5–10 min	30 min
Secretin[b]	+/–	++++	10 p*M* to 600 n*M*	~ 5 min	6–8 h
VIP	+/–	++++	75 p*M* to 100 n*M*	~ 5 min	2–3 h
pH 7.6–8.0	+/–	+++	N/A	15–30 min	ND

N/A = Not applicable; ND = not determined.

[a] Porcine glucagon (Sigma; G 3157).

[b] Porcine secretin (Sigma; S 0137).

Table 2. Negative fluid transport of PICM-19 biliary ductules in response to various agents or reduced pH

Agents	Biliary ductules	Dosage tested	Response time, min	Duration of response
Gastrin	++++	1 μ*M*	30–40	hours
Somatostatin	++++	0.5 μ*M*	30–40	hours
Epinephrine	++++	100 μ*M* to 1 m*M*	20–30	hours
Isoproterenol	++++	100 μ*M* to 1 m*M*	20–30	ND
Phenylephrine	++++	100 μ*M* to 1 m*M*	20–30	ND
pH 7.0–7.2	+++	N/A	60–90	ND

N/A = Not applicable; ND = not determined.

(1 μg/ml), however, had no visible effect on the PICM-19 ductules (table 3). Somatostatin (0.5 μ*M*)) and gastrin (1 μ*M*) caused marked reduction or total disappearance of ductal lumens in 30–60 min when the peptides were applied to ducts that were already spontaneously inflated (table 2). However, neither somatostatin (0.5 μ*M*) nor gastrin (1 μ*M*) was effective in reversing the secretin-induced (100 n*M*) ductular distension. Treatment of the ductules with adrenergic agonists, epinephrine, isoproterenol and phenylephrine (100 μ*M*) resulted in the complete shrinkage of ductal lumens in 20–30 min (table 2). Similar responses were elicited in the ductular structures produced in vitro from secondary cultures of pig liver-derived bile duct epithelium (table 4).

TEM of PICM-19 in vitro Ductules

As previously reported [Talbot et al., 1996] for standard pH culture conditions (pH 7.3–7.4), the PICM-19 multicellular ductal structures induced by elevated pH culture conditions (pH 7.6–7.8) were long tubes with well-defined lumens. In cross section, lumens were formed by the apposition of several PICM-19 cells arranged in a circle and joined near their apical (lumenal) surfaces by tight junctions and desmosomes [Talbot et al., 1996] (fig. 7, 9). Dozens of individual lumens were examined by TEM before and after exposure to secretin. In all cases, the lumens had expanded dramatically after 10 min exposure to 100 n*M* secretin (compare fig. 7A, B). The densely staining material found in the uninflated lumens (fig. 7A) was apparently diluted by the rapid transport of fluid into the duct following exposure to secretin. Only widely scattered remnants of the material could be seen within the greatly expanded lumens (fig. 7B).

Several significant ultrastructural features not previously reported were found in the ductular cells. The ducts were usually sandwiched in between an upper and lower layer of STO feeder cells and collagen fibrils were common between the basal aspect of the PICM-19 cells

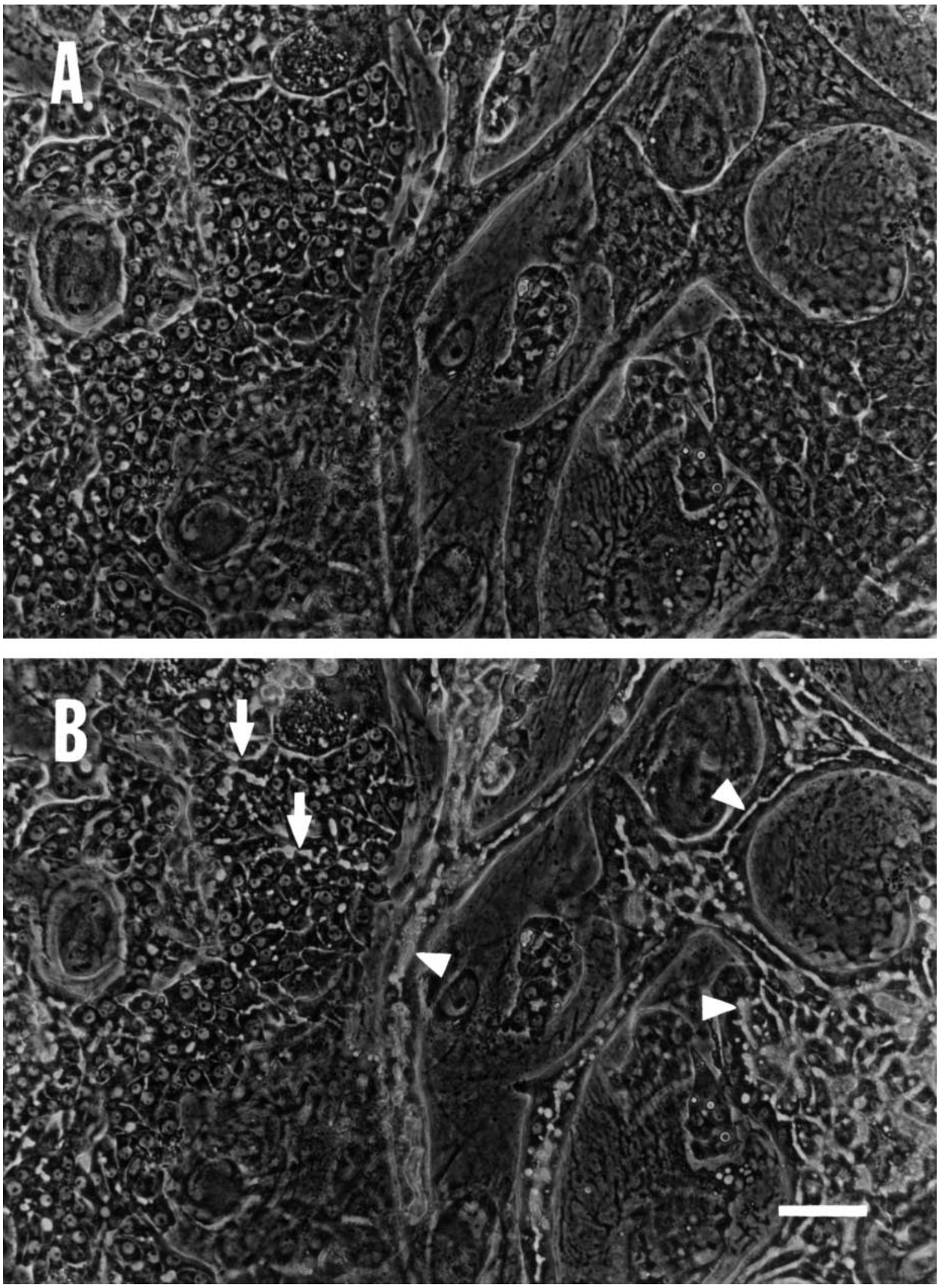

4

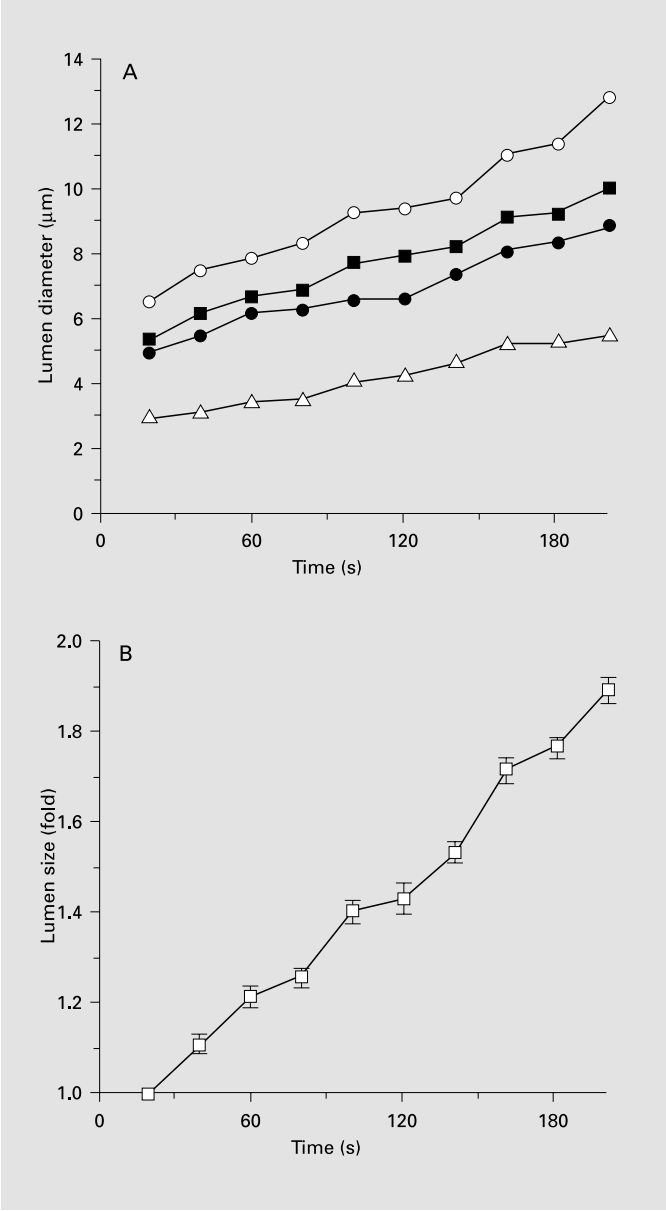

Fig. 4. (Opposite page) Phase-contrast micrographs of the response of PICM-19 hepatocyte-like cell monolayers and ductal structures to a cAMP inducer. A Cells before treatment with forskolin. B Cells 20 min after the addition of the 10 μ*M* forskolin. Note the formation of new biliary canaliculi between the hepatocyte-like cells (arrows) and the expansion of the ductal structure lumens (arrowheads). Bar ≈60 μm.

Fig. 5. (Above) PICM-19 ductule lumen enlargement after exposure to 100 n*M* secretin. A Time course of diameter enlargement in a PICM-19 duct measured at 4 locations along its length beginning 30 s after exposure to secretin. Maximal response was reached by 3–4 min. B Same data presented in A, but plotted as a ratio compared to its starting diameter. Note that the lumen diameter doubled in size.

and the STO feeder cells (fig. 7A, B). Cilia were found protruding into the lumens of the ducts, i.e. they were observed in almost every lumen examined. Their internal microtubule structure was clearly shown and they were cut at various angles and to different extents along their lengths (fig. 7B, C). However, cilia were apparently rare, probably occurring as monocilia or oligocilia, as no basal bodies were found after careful examination of six grids with 3–4 full length (i.e., traversing the grid) sections per grid. The ductule cells extensively interdigitated along their lateral surfaces and interconnective filaments were frequently seen running beneath the apical cytoplasmic membrane (fig. 9). The nuclei of the cells were oval and were often seen to be slightly crenulated (fig. 7). Rough endoplasmic reticulum was particularly well represented in the cells and was sometimes found in extensive stacked swirls (fig. 8). Golgi complexes, which were usually found in a supranuclear position, were usually not extensively developed (fig. 9). Mitochondria were elongate (2–3 μm in length) in longitudinal section and oval (0.2–0.3 μm in diameter) in cross section (fig. 9). Their lamellar cristae characteristically traversed the mitochondrion and electron-dense granules were sometimes present within their matrixes (fig. 9). Two unidentified membrane-bound bodies were also observed. The first of these, which occurred quite frequently, resembled peroxisomes [Bulger, 1983; Jones and Spring-Mills, 1983]. They were similar in size or larger than the surrounding mitochondria and they were frequently associated with smooth endoplasmic reticulum. Also, they often had laterally disposed prismatic structures resembling marginal plates or crystalline nucleoids that occasionally completely filled the body (fig. 8). The other unidentified cytoplasmic body was similar in appearance to membrane-bound very-low-density lipoprotein granules [Weiss, 1983] and was approximately 0.05–0.1 μm in diameter (fig. 9).

Western Blot Analysis for Aquaporin-1 and Aquaporin-9, and Cytokeratin-7 during PICM-19 Ductular Differentiation

PICM-19 cells were assayed for the expression of aquaporin-1 and aquaporin-9, and cytokeratin-7 during their differentiation into multicellular ductal structures under pH 7.6–7.8 culture conditions. The PICM-19 cultures were maintained in static culture to allow differentiation for 10 days (1.5 weeks), 3 weeks, and 10 weeks postpassage before being harvested for total proteins. The expression of the aquaporins and cytokeratin-7 were compared with equally loaded protein samples from STO feeder cells only, adult pig bile duct tissue, adult pig liver tissue,

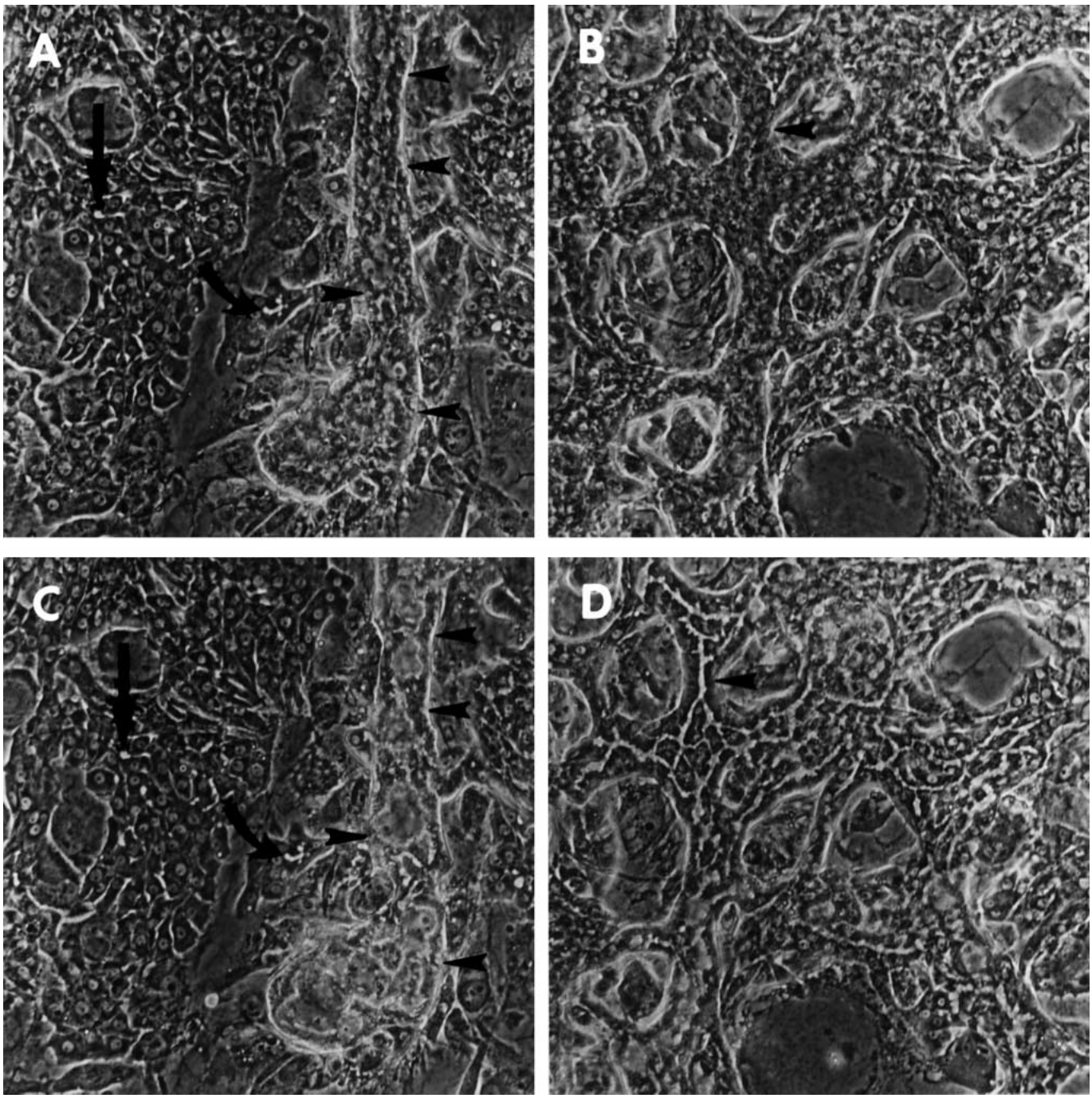

Fig. 6. Phase-contrast micrograph of secretin response in PICM-19 cells cultured at pH 7.6–7.8 for 3–4 weeks. The cells have formed multicellular ductal structures (arrowheads), but also have monolayer areas of cuboidal hepatocyte-like cells connected by canaliculi (arrows, A, C). A, B Culture before the addition of secretin. C, D The same areas, respectively, 10 min after the addition of 500 n*M* secretin. Note the swelling of the ductal lumens as fluid is transported into the ducts (C, D) in response to secretin, and, in contrast, the lack of change in the canaliculi between the hepatocyte-like cells. × 160.

Fig. 7. (Opposite page) Transmission electron micrograph of PICM-19 ductal structures. One was fixed prior to (A) and the other after (B) exposure to 100 n*M* secretin for 10 min. Note the expansion of the lumenal area in response to secretin (B). × 4,300. Inset (C) is from B as indicated by the arrowhead in the ductal lumen, and it

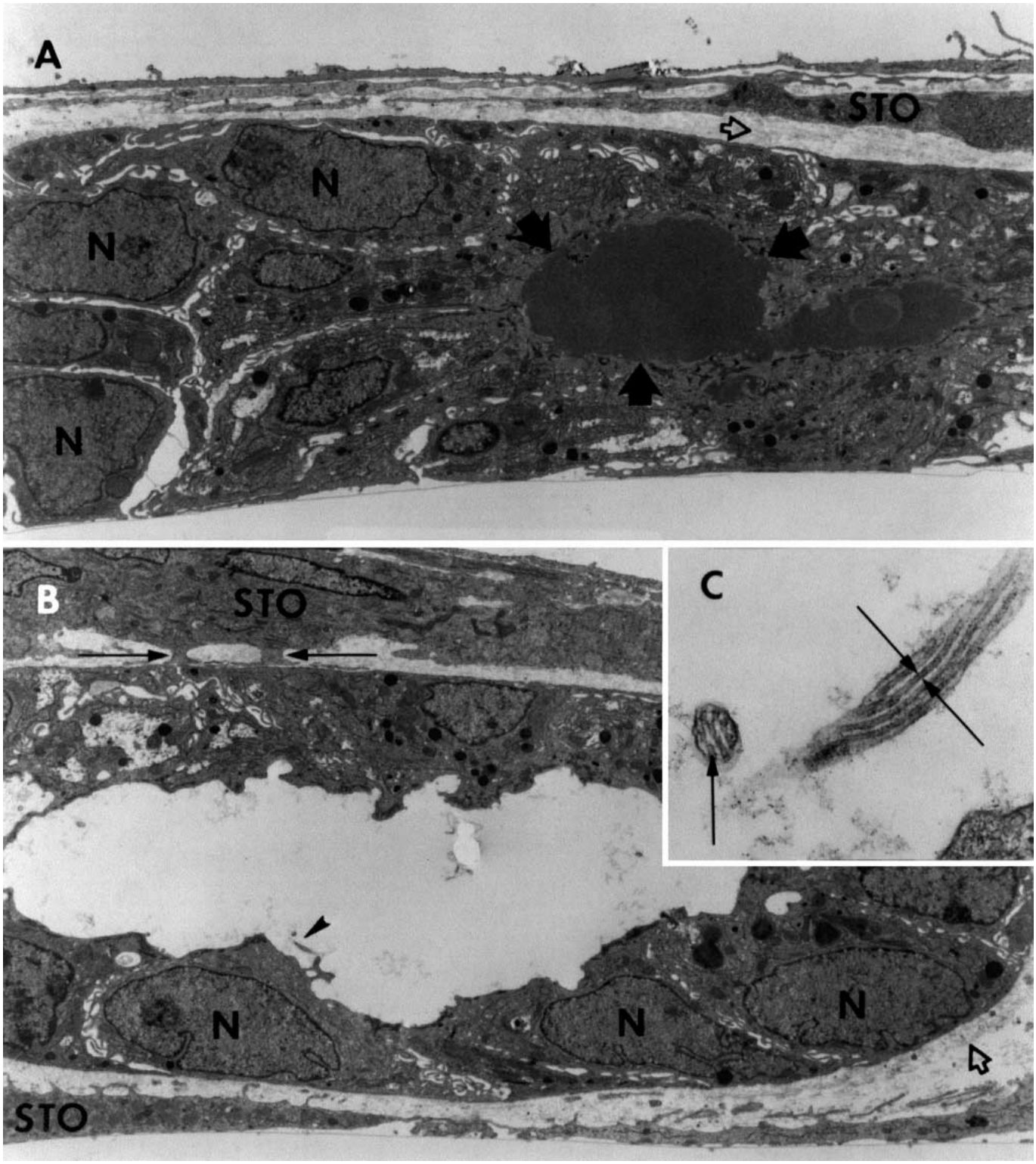

7

shows a higher magnification (53,000×) of the cilia projecting into the lumen of the duct. A The large solid arrows indicate the collapsed ductal lumen filled with an electron-dense staining material, and the small open arrow (also in B) indicates the collagen fiber matrix produced by the STO feeder cells that have moved over the top of the ductal structure. B The long arrows indicate short STO pseudopods nearly touching the PICM-19 cells. Note the STO feeder cells in their typical arrangement above and below the PICM-19 ductal structure. C Note the microtubules of the cilia, cut in cross section and tangentially (arrows).

Table 3. Noneffectors of PICM-19 biliary canaliculi and ductules

Peptides/ cAMP inducers	Biliary canaliculi	Biliary ductules	Dosage tested	Duration of test observation, h
CCK-8[a]	–	–	1–10 μ*M*	2
Bombesin	–	–	1–10 μ*M*	2–3
Endothelin-1	–	–	1–3 μg/ml	2–3
Neuropeptide Y	–	–	0.1–1 μ*M*	2
Vasopressin[b]	–	–	1 IU	2

[a] [Tyr(SO_3H^{27})]-cholecystokinin amide, fragment 26–33 (Sigma No. C-2175).
[b] [Arg^8]-vasopressin 100 IU/ml (Sigma No. V-0377).

Table 4. Response to bioactive peptide, cAMP inducers, and pH of adult pig liver-derived bile duct cell culture ductules

Peptides/pH/ cAMP inducers	Biliary ductules	Dosage tested	Response time	Duration of test observations, h
Lumen expansion response				
Glucagon[a]	+++	1 μ*M*	10–20 min	2
Secretin[b]	++++	100 n*M*	~ 5 min	2
VIP	++++	100 n*M*	~ 5 min	2
Forskolin	++++	10 μ*M*	10–20 min	2
pH 7.6–7.8	++	N/A	20–30 min	1
Lumen reduction response				
Somatostatin	+++	1.0 μ*M*	60–90 min	2
pH 7.0	+++	N/A	1–2 h	3
Lumen nonresponse				
CCK-8[c]	–	3 μ*M*	N/A	2
Bombesin	–	10 μ*M*	N/A	2–3
Endothelin-1	–	3 μg/ml	N/A	2–3

N/A = Not applicable.
[a] Porcine glucagon (Sigma; G 3157).
[b] Porcine secretin (Sigma; S 0137).
[c] [Tyr(SO_3H^{27})-cholecystokinin amide, fragment 26–33 (Sigma No. C-2175).

and adult pig red blood cells (fig. 10). At 1.5 weeks postpassage the PICM-19 cultures showed little expression of any of the proteins (fig. 10, lane 1). However, by 3 weeks postpassage, in which time ductal structures are maturing, the presence of all three proteins was found in the PICM-19 cultures (fig. 10, lane 2). By 10 weeks postpassage ductal structures have long been fully mature and 75% or more of the PICM-19 cells were participating in this phenotype within the culture. The three proteins were again detected at this late time point, and they appeared to be at higher concentrations than at the 3-week time point (fig. 10, lane 4). STO feeder cells alone did not express the proteins (fig. 10, lane 3), and the expression from pig liver tissue was specific to bile duct tissue (fig. 10, lanes 5 and 6). As expected, aquaporin-1 was also abundant in RBC membranes (fig. 10, lane 7). The estimated molecular weights of the pig proteins assayed were 26 kD for aquaporin-1, 42 kD for the major band of aquaporin-9, and 41–48 kD for cytokeratin-7.

Fig. 8. Transmission electron micrograph of PICM-19 ductular cell showing an extensive array of endoplasmic reticulum and several peroxisome-like bodies with prismatic marginal plates (arrows). × 50,000. Inset is of another peroxisome-like body, apparently connecting to the endoplasmic reticulum (arrows), whose internal space is nearly filled by a highly ordered crystalloid structure. × 130,000.

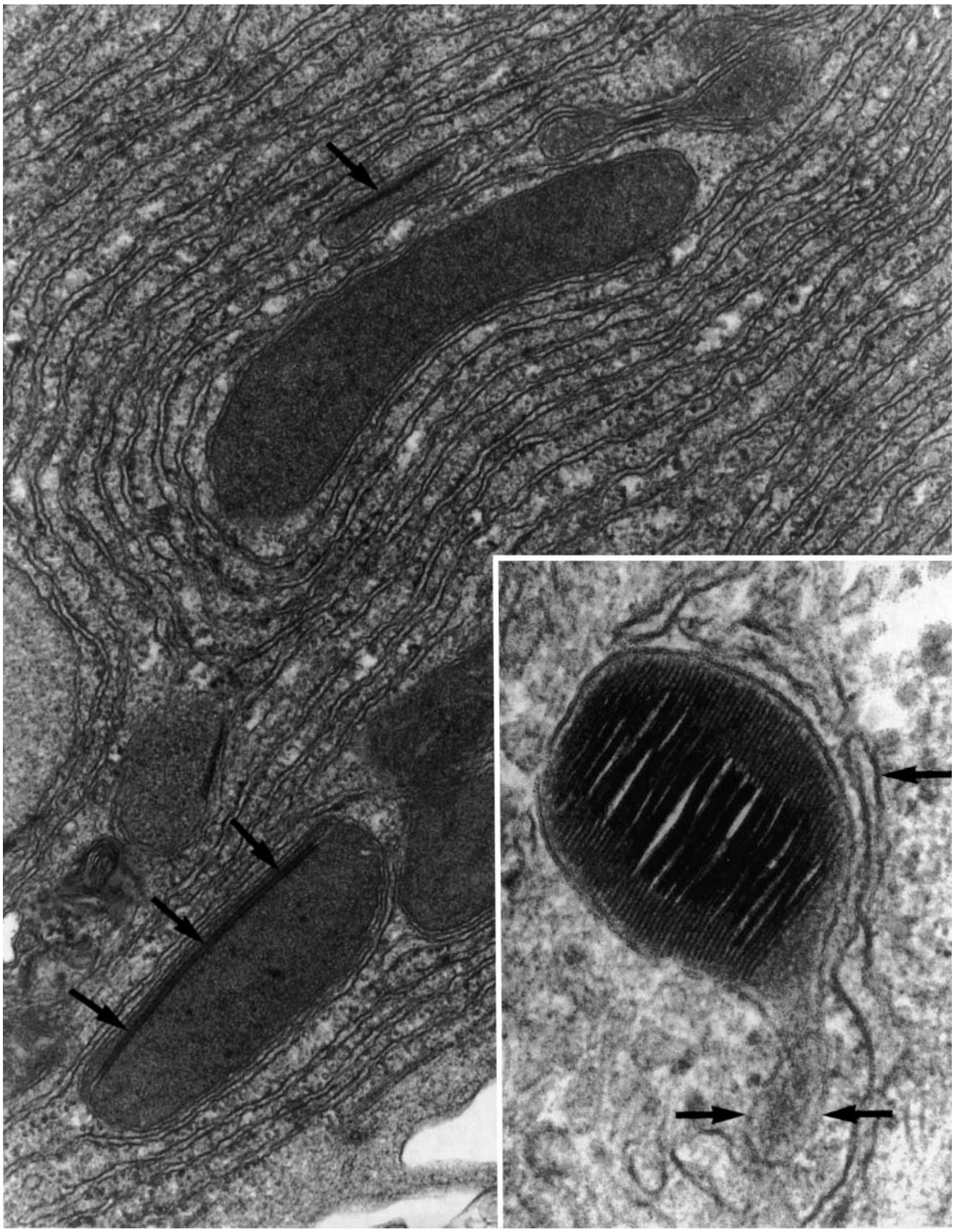

8

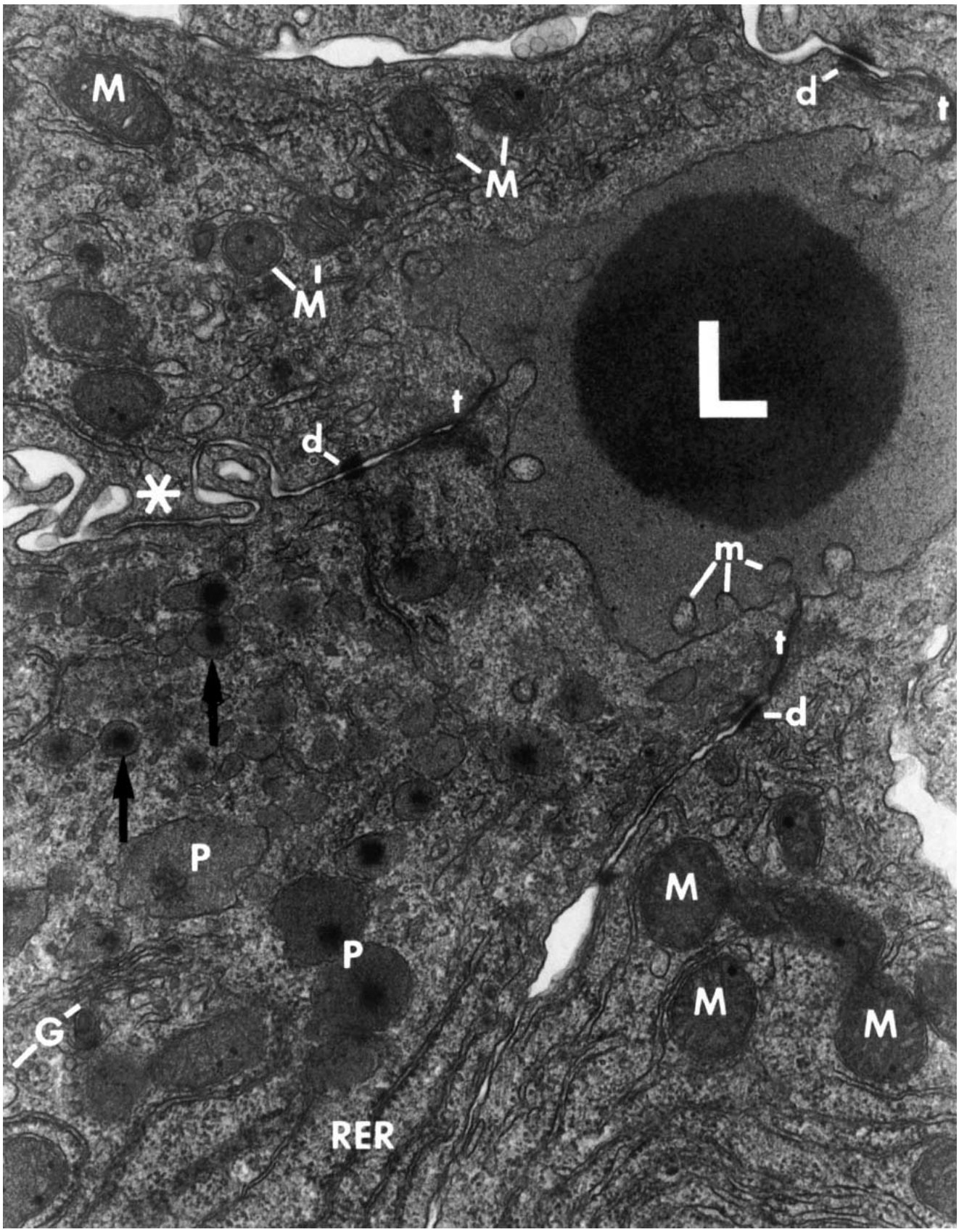

9

Discussion

The data presented show that the PICM-19 cells grown at elevated pH expressed markers of bile duct epithelium as they differentiated into ductal structures. That is, PICM-19 cells at 10 days postpassage were negative for the expression of cytokeratin-7, and aquaporin-1 and aquaporin-9 (fig. 10), known markers for bile duct epithelium [Van Eyken and Desmet, 1993; Roberts et al., 1994]. However, as differentiation proceeded, i.e. ductal formations organized, the cultures were found to express the proteins, and this expression was heightened as ductular differentiation increased and matured over further time postpassage. Some of this increase in signal over time may be the result of further cell division after the initial 10 days of culture, but it is probably mostly the result of differentiation because the cells dramatically slow their cell division after 10 days. This is evident from the fact that the cells never approach 100% confluency, even after months of culture, but instead terminally differentiate (fig. 1) [Talbot et al., 1994a].

Functional evidence of the bile duct character of the PICM-19 cells was the induced transport of fluid into and out of the ducts in response to direct stimulation of cAMP and cGMP levels [Kato et al., 1992; Mennone et al., 1995; Myers et al., 1996], or in response to bioactive peptides known to work either through cAMP [Lenzen et al., 1990; Roberts et al., 1993; Mennone et al., 1995; Tietz et al., 1995] or not [Cho, 1997; Cho and Boyer, 1999] in stimulating or inhibiting bile duct secretion. These included forskolin and bcAMP, which stimulated fluid transport into both ductal structures and canaliculi (between monolayer hepatocyte-like cells) in 15–20 and 30–60 min, respectively, and cGMP which stimulated canalicular transport after 90 min. Bioactive peptides such as secretin, vasoactive intestinal peptide (VIP), and glucagon stimulated maximal ductal expansion a little faster (5–10 min), and this response time was similar to that pre-

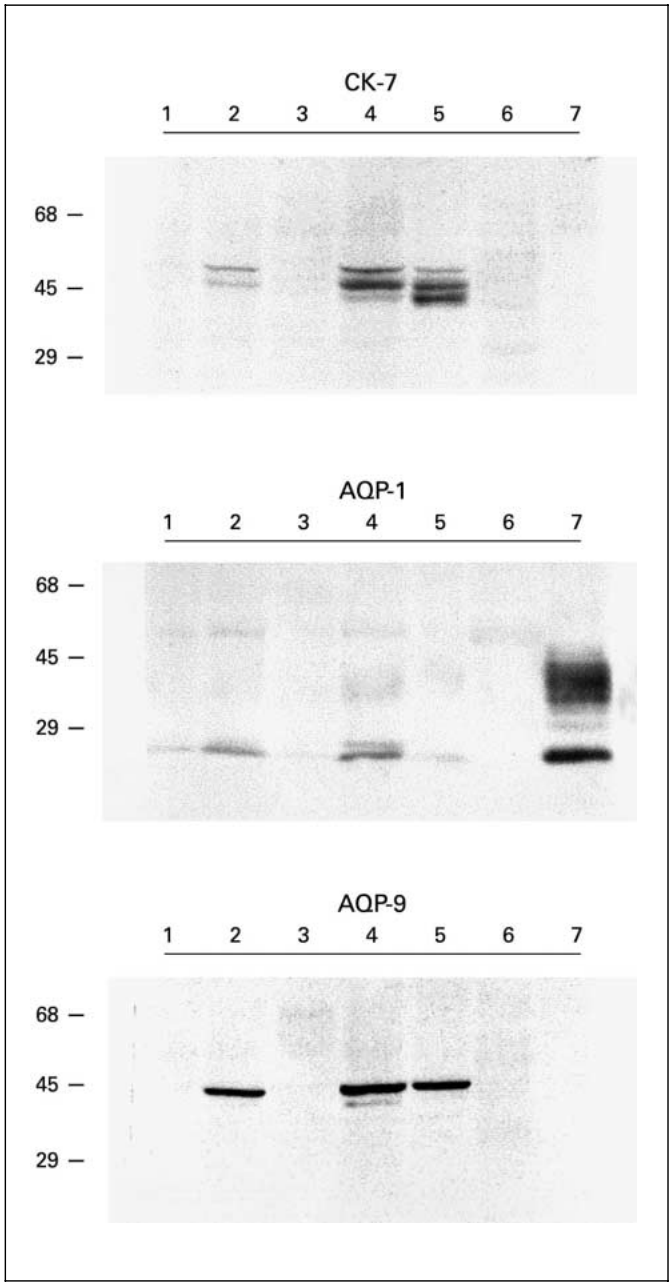

10

Fig. 9. (Opposite page) Transmission electron micrograph of collapsed ductal lumen formed by several PICM-19 cells. Note the tight junctions (t) and their associated desmosomes (d) joining the cells together at their apical (lumenal) aspect. Also, note the interdigitations (*) of the lateral membranes closely associating the cells to each other. The lumen (L) is filled with a densely staining substance and microvilli (m) protrude into the lumen. Rough endoplasmic reticulum (RER) is present along with Golgi complex (G), peroxisome-like bodies (P), secretory granules (arrows), and numerous mitochondria (M) with granular inclusions in their matrixes. × 35,000.

Fig. 10. Western immunoblot analysis of intracellular proteins in cultures of PICM-19 cells. Cellular material was prepared from STO control cultures (lane 3) or co-cultures of PICM-19 cells at 1.5 weeks (lane 1), 3 weeks (lane 2) or 10 weeks (lane 4) and membranes were prepared from normal porcine tissues, i.e. cystic/bile duct (lane 5), whole liver (lane 6) and red blood cells (lane 7). Note the increase in expression of all the proteins assayed over time postpassage, i.e. in correlation with the increasing differentiation or maturation of the PICM-19 ductal structures. Also, note the concordance in phenotype between the PICM-19 ductular cultures and in vivo pig bile duct tissue samples. AQP = Aquaporin.

viously observed in rodent cholangiocytes, liver-derived bile duct units, and in vivo bile ducts [Lenzen et al., 1990; Kato et al., 1992; Farouk et al., 1993; Mennone et al., 1995; Tietz et al., 1995]. An opposite physiological-like response was elicited by peptides previously shown to decrease bile secretion. That is, the application of gastrin or somatostatin to the cell cultures caused the PICM-19 ductules to close down or apparently lose fluid from their lumens [Tietz et al., 1995; Glaser et al., 1997]. Similarly, catecholamines, specifically the adrenergic agonists, epinephrine, isoproterenol, and phenylephrine, that have been shown to have negative effects on biliary secretion, caused fluid transport out of the PICM-19 ductules [Krell et al., 1985]. Also, this report may be unique in its direct demonstration of the effects of external pH on the fluid transport of bile duct epithelium. Although these pH effects were caused by pH conditions that were probably outside the physiological range, particularly the acid load, their occurrence demonstrates the potential utility of the PICM-19 culture system for investigating the dynamics of Na^+, K^+, H^+, Cl^-, and HCO_3^- exchange in itself and in response to specific peptides in bile duct epithelium [Strazzabosco, 1997].

Variation in the responsiveness of the canaliculi of the hepatocyte-like cells versus ductal structures may reflect the transitional morphological and biochemical continuum that exists between hepatocytes and intrahepatic bile ductule cells within the liver [Sternlieb, 1972; Jungermann and Katz, 1989]. Similarly, differences in responsiveness to specific peptides such as secretin and glucagon within the bile duct network have been demonstrated [Lenzen et al., 1990; Alpini et al., 1997]. This morphological continuum appears to also exist in vitro in the PICM-19 culture where cells of hepatocyte morphology sometimes seamlessly connect to cells of bile duct morphology [Talbot et al., 1994a]. Such variation may be functionally reflected in the different responses found amongst the PICM-19 cells. For example, secretin, VIP and glucagon stimulated biliary canaliculi between monolayer hepatocyte-like PICM-19 cells either not all or in a slower response (30–90 min). In contrast, bcGMP stimulated fluid transport only in canaliculi and not in ductal structures. Also, of interest was the variation in the duration of responses (table 1). For example, glucagon-stimulated fluid transport was a transitory response that lasted less than 1 h even in the continuous presence of the peptide, whereas secretin-stimulated fluid transport was maintained for several hours even after thorough washing of the cells to remove the peptide. Thus, the PICM-19 cell culture may reproduce some aspects of the morphological and functional variation seen in the intact liver.

The lack of response of the PICM-19 cells to other agents known to increase or inhibit bile secretion, i.e. bombesin, neuropeptide Y, CCK-8, vasopressin and endothelin-1 [Kaminski et al., 1988; Ballatori and Truong, 1990; Cho, 1997; Yoneda et al., 1997; Caligiuri et al., 1998], is notable. However, a similar lack of response was seen in in vitro-produced ductal structures from bile duct epithelium cells derived from adult pig liver tissue (table 4) [Talbot et al., 1998]. Therefore, this apparent deficiency in the PICM-19 bile duct model is not inherent to the PICM-19 cells themselves and is apparently not related to their fetal phenotype. Bombesin appears to stimulate secretion from cholangiocytes directly, assuming that no accessory stromal cells or neuronal cells are intimately associated with isolated bile duct units [Cho, 1997]. If this assumption is correct, then it is probable that some component of the bombesin signal pathway has been perturbed in the PICM-19 ductules as a result of in vitro growth and differentiation. This could involve either changes within the cells themselves, e.g. specific receptor downregulation, or might result from the lack of a necessary synergism with other cell surface, paracrine or endocrine factors. Similar arguments could be made for endothelin-1 which failed to cause the collapse of PICM-19 ductules despite having been shown to inhibit bile ductule secretion directly in isolated bile duct units from rat liver [Caligiuri et al., 1998]. In contrast, CCK-8 and neuropeptide Y may very well induce biliary secretory responses indirectly, i.e. through other cells associated with the bile ductules such as endothelium, smooth muscle or neuronal cells, or by induction of other effector peptides in other tissues [Kaminski et al., 1988; Yoneda et al., 1997].

The possible mechanisms underlying the pH-mediated induction of preferential differentiation of the PICM-19 cells into ductular structures can only be speculated upon at this point. It could be a direct effect whereby the PICM-19 cells are solely affected, e.g., gap junction communication can be influenced by pH [Lee and Rhee, 1998; Bevans and Harris, 1999]. Conversely or in addition, the cause may be indirect, i.e., the interaction between the STO feeder cells and the PICM-19 cells may mediate the preference to form ductular structures. For example, pH could effect the constitution of the STO matrix since matrix serine proteinase proenzyme activation and subsequent activity are pH responsive [Coleman et al., 1982; Koshikawa et al., 1992], or the recent elucidation of soluble adenylyl cyclase as a bicarbonate-responsive enzyme may have relevance [Chen et al., 2000].

This is the first report to demonstrate the expression of aquaporins in pig bile duct tissue, and the rapid fluid

transport into the PICM-19 ductules is probably mediated by them as it is in rodent bile duct cells [Marinelli et al., 1999]. The lack of inhibition by colcemid may indicate that sufficient aquaporin proteins are chronically inserted into the apical membranes of the PICM-19 cells so that immediate microtubule-mediated insertion is not required as reported by Marinelli et al. [1999]. Whether this is a species difference, pig versus rat [Marinelli et al., 1999], a characteristic of PICM-19 that is fetal in phenotype [Talbot et al., 1994a], or a difference resulting from in vitro culture conditions is unknown.

The TEM analysis of the cells demonstrated a key feature typical of bile duct epithelium. That is, the cells were ciliated as evidenced by the presence of cilia, cut in various planes, in the lumens of the ductal structures. Since connections to basal bodies were not observed, i.e. were very rare, despite the examination of dozens of ductular cross sections, the cells are probably monociliated or oligociliated as previously reported for pig bile duct cells [Singh and Shahidi, 1987; Talbot et al., 1998]. The relatively large unidentified membrane-bound bodies frequently found in the cells may be peroxisomes. This is likely since they appeared to vary considerably in size, had a fine granular matrix without cristae structures, occurred in association with smooth endoplasmic reticulum and often had laterally disposed prismatic structures resembling marginal plates [Bulger, 1983] (fig. 8) or dramatically laminated cores or nucleoids [Jones and Spring-Mills, 1983] (fig. 8) that are common in pig hepatocytes [Singh and Shahidi, 1987]. The cells' nuclei were also typical of bile duct cells in being slightly oblong and crenulated instead of the evenly round nuclei typical of hepatocytes [Jones and Spring-Mills, 1983; Sirica et al., 1985]. Finally, the overall structure of the PICM-19 ductules with their circularly arranged cuboidal cells surrounded by a collagen fiber matrix was similar to that observed in vivo [Jones and Spring-Mills, 1983; Singh and Shahidi, 1987]. However, a basement membrane, which is normally present in vivo, was not an obvious feature of the PICM-19 in vitro ductules.

In summary, the PICM-19 cell line is unique in several respects. It originated from the spontaneous differentiation of pig epiblast tissue and is therefore derived from pig embryonic stem cells [Talbot et al., 1993, 1994a]. The cell line is also unique in its characteristic differentiation into two phenotypes that resemble fetal hepatocytes or fetal and adult bile duct epithelium [Talbot et al., 1994b, 1996, 1998]. The second of these phenotypes, bile duct epithelium, is manifested by a unique and striking in vitro morphological change, i.e. the formation of multicellular ductal structures [Talbot et al., 1994a, 1996]. Besides their evident morphological similarity to multicellular ductal structures shown also to occur in cell cultures derived from pig fetal liver tissue and adult liver tissue [Talbot et al., 1994b, 1998], the PICM-19 cells have previously been shown to express GGT strongly at their apical (lumenal) cell membranes. GGT is a well-known enzymatic marker of bile duct epithelium [Tanaka, 1974; Ishii et al., 1989]. This report demonstrates another unique property of the cell line, i.e. that is differentiation into multicellular ductal formations can be preferentially induced by culturing the cells at pH 7.6–7.8. It also provides further evidence of their bile duct character which is important since their derivation from embryonic stem cells carries a higher burden of proof. Since PICM-19 is clonable, it offers an opportunity for genetic manipulation of the cells to test the effects of changes in specific gene expression on the differentiation and function of bile duct epithelium. Also, the cell line offers an in vitro method for the consistent production of long-lived bile ductules whose functions can be probed through physical manipulation, e.g. micropipet techniques, or through manipulation of the culture environment.

Acknowledgments

We thank Dr. John P. McMurtry, Dr. Delores Lana, Dr. John M. Talbot, and Dr. Vernon G. Pursel for reading the manuscript and offering helpful editorial and scientific comments in its final preparation.

References

Alpini, G., S. Glaser, W. Robertson, R.E. Rodgers, J.L. Phinizy, J. Lasater, G.D. LeSage (1997) Large but not small intrahepatic bile ducts are involved in secretin-regulated ductal bile secretion. Am J Physiol *272:* G1063–G1074.

Ballatori, N., A.T. Truong (1990) Cholestasis, altered junctional permeability, and inverse changes in sinusoidal and biliary glutathione release by vasopressin and epinephrine. Mol Pharmacol *38:* 64–71.

Bevans, C.G., A.L. Harris (1999) Regulation of connexin channels by pH. J Biol Chem *274:* 3711–3719.

Bulger, R.E. (1983) The urinary system; in Weiss, L. (ed): Histology: Cell and Tissue Biology, ed 5. New York, Elsevier Biomedical, p 888.

Caligiuri, A., S. Glaser, R.E. Rodgers, J.L. Phinizy, W. Robertson, E. Papa, M. Pinzani, G. Alpini (1998) Endothelin-1 inhibits secretin-stimulated ductal secretion by interacting with ETA receptors on large cholangiocytes. Am J Physiol *275:* G835–G846.

Chen, Y., M.J. Cann, T.N. Litvain, V. Iourgenko, M.L. Sinclair, L.R. Levin, J. Buck (2000) Soluble adenylyl cyclase as an evolutionarily conserved bicarbonate sensor. Science *289:* 625–628.

Cho, W.K. (1997) Role of the neuropeptide, bombesin, in bile secretion. Yale J Biol Med *70:* 409–416.

Cho, W.K., J.L. Boyer (1999) Vasoactive intestinal polypeptide is a potent regulator of bile secretion from rat cholangiocytes. Gastroenterology *117:* 420–428.

Coleman, P.L., P.A. Barouski, T.D. Gelehrter (1982) The dexamethasone-induced inhibitor of fibrinolytic activity in hepatoma cells. J Biol Chem *257:* 4260–4264.

Farouk, M., S.R. Vigna, J.E. Haebig, T.W. Gettys, D.C. McVey, R. Chari, R.S. Pruthi, W.C. Meyers (1993) Secretin receptors in a new preparation of plasma membranes from intrahepatic biliary epithelium. J Surg Res *54:* 1–6.

Glaser, S.S., R.E. Rodgers, J.L. Phinizy, W.E. Robertson, J. Lasater, A. Caligiuri, Z. Tretjak, G.D. LeSage, G. Alpini (1997) Gastrin inhibits secretin-induced ductal secretion by interaction with specific receptors on rat cholangiocytes. Am J Physiol *273:* G1061–G1070.

Ishii, M., B. Vroman, N.F. LaRusso (1989) Isolation and morphologic characterization of bile duct epithelial cells from normal rat liver. Gastroenterology *97:* 1236–1247.

Jones, A.L., E. Spring-Mills (1983) The liver and gallbladder; in Weiss, L. (ed): Histology: Cell and Tissue Biology, ed 5. New York, Elsevier Biomedical, p 737.

Kaminski, D.L., Y.G. Deshpande, M.C. Beinfeld (1988) Role of glucagon in cholecystokinin-stimulated bile flow in dogs. Am J Physiol *254:* G864–G869.

Kato, A., G.J. Gores, N.F. LaRusso (1992) Secretin stimulates exocytosis in isolated bile duct epithelial cells by a cyclic AMP-mediated mechanism. J Biol Chem *267:* 15523–15529.

Koshikawa, N., H. Yasumitsu, M. Umeda, K. Miyazaki (1992) Multiple secretion of matrix serine proteinases by human gastric carcinoma cell lines. Cancer Res *52:* 5046–5053.

Krell, H., H. Jaeschke, E. Pfaff (1985) Regulation of canalicular bile formation by α-adrenergic action and by external ATP in the isolated perfused rat liver. Biochem Biophys Res Commun *131:* 139–145.

Jungermann, K., N. Katz (1989) Functional specialization of different hepatocyte populations. Physiol Rev *69:* 708–764.

Lee, M.J., S.K. Rhee (1998) Heteromeric gap junction channels in rat hepatocytes in which the expression of connexin-26 is induced. Mol Cell *8:* 295–300.

Lenzen, R., V.J. Hruby, N. Tavoloni (1990) Mechanism of glucagon choleresis in guinea pigs. Am J Physiol *259:* G736–G744.

Marinelli, R.A., P.S. Tietz, L.D. Pham, L. Rueckert, P. Agre, N.F. LaRusso (1999) Secretin induces the apical insertion of aquaporin-1 water channels in rat cholangiocytes. Am J Physiol *276:* G280–G286.

Mennone, A., D. Alvaro, W. Cho, J.L. Boyer (1995) Isolation of small polarized bile duct units. Proc Natl Acad Sci USA *92:* 6527–6531.

Myers, N.C., S. Grune, H.L. Jameson, M. Sawkat-Anwer (1996) cGMP stimulates bile acid-independent bile formation and biliary bicarbonate excretion. Am J Physiol *270:* G418–G424.

Nerurkar, L.S., P.A. Marino, D.O. Adams (1981) Quantification of selected intracellular and secreted hydrolases of macrophages; in Herskowitz, H.B., H.T. Holden, J.A. Bellanti, A. Ghaffar (eds): Manual of Macrophage Methodology. New York, Dekker, pp 229–247.

Roberts, K.S., S.M. Kuntz, G.J. Gores, N.F. LaRusso (1993) Regulation of bicarbonate-dependent ductular bile secretion assessed by lumenal micropuncture of isolated rodent intrahepatic bile ducts. Proc Natl Acad Sci USA *90:* 9080–9084.

Roberts, S.K., M. Yano, Y. Ueno, L. Pham, G. Alpini, P. Agre, N.F. LaRusso (1994) Cholangiocytes express the aquaporin CHIP and transport water via a channel-mediated mechanism. Proc Natl Acad Sci USA *91:* 13009–13013.

Singh, A., E. Shahidi (1987) Ultrastructure of piglet liver; in Tumbleson, M.E. (ed): Swine in Biomedical Research. New York, Plenum Press, vol 1, p 84.

Sirica, A.E., C.A. Sattler, H.P. Chila (1985) Characterization of a primary bile ductular cell culture from the livers of rats during extrahepatic cholestasis. Am J Pathol *120:* 67–78.

Sternlieb, I. (1972) Special article: Functional implications of human portal and bile ductular ultrastructure. Gastroenterology *63:* 321–327.

Strazzabosco, M. (1997) Transport system in cholangiocytes: Their role in bile formation and cholestasis. Yale J Biol Med *70:* 427–434.

Talbot, N.C., T.J. Caperna (1998) Selective and organotypic culture of intrahepatic bile duct cells from adult pig liver. In Vitro Cell Dev Biol *34A:* 785–798.

Talbot, N.C., T.J. Caperna, L.T. Lebow, D. Moscioni, V.G. Pursel, C.E. Rexroad Jr. (1996) Ultrastructure, enzymatic, and transport properties of the PICM-19 bipotent liver cell line. Exp Cell Res *225:* 22–34.

Talbot, N.C., M.J. Paape (1996) Continuous culture of pig tissue-derived macrophages. Methods Cell Sci *18:* 315–327.

Talbot, N.C., M. Paape, M. Worku (1998) Selective and continuous culture of macrophages from adult pig blood. Vet Immunol Immunopathol *64:* 173–190.

Talbot, N.C., A. Powell, W. Garrett, J.L. Edwards, C.E. Rexroad Jr. (2000) Ultrastructural and karyotypic examination of in vitro produced bovine embryos developed in the sheep uterus. Tissue Cell *32:* 9–27.

Talbot, N.C., V.G. Pursel, C.E. Rexroad Jr., T.J. Caperna, A.M. Powell, R.T. Stone (1994b) Colony isolation and secondary culture of fetal porcine hepatocytes on STO feeder cells. In Vitro Cell Dev Biol *30A:* 851–858.

Talbot, N.C., C.E. Rexroad Jr., A. Powell, V.G. Pursel, T.J. Caperna, S.L. Ogg, N.D. Nel (1994a) A continuous culture of pluripotent fetal hepatocytes derived from the 8-day epiblast of the pig. In Vitro Cell Dev Biol *30A:* 843–850.

Talbot, N.C., C.E. Rexroad Jr., V.G. Pursel, A.M. Powell, N.D. Nel (1993) Culturing the epiblast cells of the pig blastocyst. In Vitro Cell Dev Biol *29A:* 543–554.

Tanaka, M. (1974) A histochemical study on the activity of gamma-glytamyl transpeptidase in liver disease. Acta Pathol Jpn *24:* 651–665.

Tietz, P.S., G. Alpini, L.D. Pham, N.F. LaRusso (1995) Somatostatin inhibits secretin-induced ductal hypercholeresis and exocytosis by cholangiocytes. Am J Physiol *269:* G110–G118.

Van Eyken, P., V.J. Desmet (1993) Cytokeratins and the liver. Liver *13:* 113–122.

Weiss, L. (1983) The cell; in Weiss, L. (ed): Histology: Cell and Tissue Biology, ed 5. New York, Elsevier Biomedical, pp 53–54.

Yoneda, M., S. Yokohama, K. Tamori, Y. Sato, K. Nakamura, I. Makino (1997) Neuropeptide Y in the dorsal vagal complex stimulates bicarbonate-dependent bile secretion in rats. Gastroenterology *112:* 1673–1680.